



# Inferring synaptic connectivity from spatio-temporal spike patterns

Frank Van Bussel<sup>1,2,3\*</sup>, Birgit Kriener<sup>1,2,4</sup> and Marc Timme<sup>1,2,3</sup>

<sup>1</sup> Network Dynamics Group, Max Planck Institute for Dynamics and Self-Organization, Göttingen, Germany

<sup>2</sup> Bernstein Center for Computational Neuroscience Göttingen, Göttingen, Germany

<sup>3</sup> Fakultät für Physik, Georg-August-Universität Göttingen, Göttingen, Germany

<sup>4</sup> Institute of Mathematical Sciences and Technology, Norwegian University of Life Sciences, Ås, Norway

## Edited by:

David Hansel, University of Paris, France

## Reviewed by:

Maoz Shamir, Boston University, USA

Valeri A. Makarov, Universidad

Complutense de Madrid, Spain

## \*Correspondence:

Frank Van Bussel, Network Dynamics

Group, Max Planck Institute for

Dynamics and Self-Organization,

Bunsenstrasse 10, 37073 Göttingen,

Germany.

e-mail: [fvb@nld.ds.mpg.de](mailto:fvb@nld.ds.mpg.de)

Networks of well-known dynamical units but unknown interaction topology arise across various fields of biology, including genetics, ecology, and neuroscience. The collective dynamics of such networks is often sensitive to the presence (or absence) of individual interactions, but there is usually no direct way to probe for their existence. Here we present an explicit method for reconstructing interaction networks of leaky integrate-and-fire neurons from the spike patterns they exhibit in response to external driving. Given the dynamical parameters are known, the approach works well for networks in simple collective states but is also applicable to networks exhibiting complex spatio-temporal spike patterns. In particular, stationarity of spiking time series is not required.

**Keywords:** networks, inverse methods, leaky integrate-and-fire neuron, irregular spiking, chaotic spiking, synchronization

## 1 INTRODUCTION

Reconstructing or reverse-engineering the exact interaction topology of coupled dynamical units has become an active area of research in different fields of biology, including genetics, ecology, and neuroscience (see Yeung et al., 2002; Makarov et al., 2005; Cadenasso et al., 2006, for recent theoretical results). In neuroscience, such efforts generally focus on establishing the *functional* or *effective* connectivity between individual neurons and different regions of the brain using methods based on correlations in the activity between the constituent parts of the network (Aertsen and Gerstein, 1985; Aertsen et al., 1989). This research has yielded many valuable results, commonly on a scale larger than the individual elements such as nerve cells and synaptic connections that make up the networks involved (Jirsa and McIntosh, 2007).

Explicit approaches that reconstruct actual connections between individual elements are more difficult in general, but where feasible they offer exact, fine-grained results, for instance by establishing the presence or absence of individual synapses. These more detailed approaches have attracted serious attention recently, triggered by the availability of large high-resolution data sets and the computational power to handle them. Noteworthy from a theoretical point of view is a method of stochastic optimization (Makarov et al., 2005) that fits a network model of spiking leaky integrate-and-fire (LIF) neurons to an oncoming data stream and thus avoids estimating parameters beforehand. The performance of this reconstruction method has been addressed for simulated, as well as real, extracellular multiunit array (MUA) recordings. The computational requirements seem however somewhat prohibitive as the largest network which Makarov et al. report having reconstructed consists of  $N = 5$  neurons.

Other studies have focused on networks of smoothly coupled units. One of the earlier results in this regard is a synchronization method presented by Yu et al. (2006). Assuming pre-knowledge of

all model parameters, a second network of the same units is set up as a model, and its interaction topology is varied via continual error minimization until it synchronizes with the original system. Via a thresholding process, the resulting topology is identified as that of the original network. This approach has been shown to perform well for networks of up to  $N = 16$  nodes. Yu and Parlitz (2008) combine the basic idea of error minimization with an intricate mechanism for driving the network to a steady state, at which point the connectivity can be recovered from the individual node dynamics. Since this technique dispenses with the need to explicitly model the connectivity of the network they are able to achieve reconstructions of significantly larger networks ( $N = 50$ ).

An alternative approach for smoothly coupled systems close to steady states (Timme, 2007) uses measurements of the collective response–dynamics under different external driving conditions. As the collective dynamics depends on both the (known) driving signals and the (unknown) interaction topology, an increasing number of driving–response experiments yields more and more restrictions on the topology. Worked out explicitly for phase-locking oscillators, the method is insensitive to details of the units' dynamics and their coupling function and a linear approximation is often sufficient to infer the topology. Hence, the experiments yield a system of linear equations that restrict the topology consistent with all experiments that is then solved to obtain the incoming connections for each unit. This approach has been successfully applied to Kuramoto oscillators, where networks of many hundreds of units were reconstructed. Assuming sparsity of the network connectivity, such reconstructions may be supplemented by an optimization step (Timme, 2007) that reduces the number of experiments needed to reconstruct up to a desired accuracy (cf. also Yeung et al., 2002; Napoletani and Sauer, 2008). Since all experimental approaches in practice have to deal with a systematic undersampling with regard

to finite measurement times and the number of neurons that can be reliably recorded, such optimization methods are likely a necessary step in any potentially useful algorithm.

Here, we present a method to explicitly reconstruct both topology and connection weights for networks of LIF neurons. LIF neurons with current-based synapses incorporate two key features of biological neurons: they integrate the input currents of their presynaptic neurons and send spikes whenever this accumulated and filtered input sufficiently depolarizes the membrane potential  $V(t)$ . Though this class of LIF neurons lacks a lot of biophysical detail such as the spike dynamics itself, voltage-dependent integration properties, or neuronal morphology, their study can help to understand biologically relevant collective dynamic states of neuronal networks, such as population rate oscillations (Brunel and Hakim, 1999; Brunel, 2000), propagation of synchronous activity volleys (Diesmann et al., 1999), or asynchronous irregular activity states (Brunel, 2000; Jahnke et al., 2009). Moreover, they are simple enough to be amenable to analytical methods and thus reveal principle insights regarding relations between network interactions and dynamics. In general, the collective dynamics of even simple networks of LIF neurons can be highly complex, depending not only on interaction topology but also on synaptic coupling strengths, local neuron parameters, and initial conditions (van Vreeswijk and Sompolinsky, 1996; Timme et al., 2002; Denker et al., 2004; Zillmer et al., 2009).

The method presented here is in part an extension to pulse-coupled, spiking units of the driving–response approach for smoothly coupled phase-oscillators given by Timme (2007). In particular, it uses the information provided by spike times and model parameters only. Moreover, the method developed here does not require steady states as in Timme (2007) or Yu and Parlitz (2008), but works as well for complex spatio-temporal activity, such as irregular or even chaotic spiking, given that certain technical conditions are met. The robust optimization technique (Yeung et al., 2002; Timme, 2007; Napoletani and Sauer, 2008) can be applied here as well, to reconstruct networks of several hundred nodes from a comparably small number of experiments with only a small loss of accuracy.

Biological neuronal networks naturally present much more challenging problems for reconstruction than moderately sized networks of model neurons. The technique presented here should hence not be considered as a substitute to current approaches that work with spiking data from experiments, but as a theoretical complement. This notwithstanding, it has the advantage that it does not depend on continual access to the actual membrane potentials. Since in practice intracellular recordings from a large group of neurons are still beyond technical feasibility, in general any method that restricts itself to spike time data has strong merits. In this sense it presents a necessary first step toward a robust explicit method that could be used in tandem with larger-scale statistical methods.

In Section 2 we will provide necessary definitions and derivations for the LIF neuron, and then outline the basic method as it applies to exact data and known model parameters. In Section 3 we will discuss implementation and performance of the method in several contexts such as algorithmic efficiency, data requirements, and the effect of noise and uncertainty on reconstruction accuracy. In Section 4 possible extensions and applications of the method will be noted.

## 2 NEURON MODEL AND RECONSTRUCTION THEORY

### 2.1 DYNAMICS AND COLLECTIVE SOLUTION BETWEEN SUBSEQUENT SPIKES

The subthreshold dynamics of the membrane potential  $V_i(t)$  of a LIF neuron  $i$  is given by the linear ordinary differential equation

$$\frac{dV_i(t)}{dt} = \gamma_i (R_i I_i(t) - V_i(t)) + S_i(t), \quad (1)$$

where  $\gamma_i$  is the inverse of the membrane time constant,  $R_i$  is the membrane resistance,  $I_i(t)$  is a temporally constant, externally applied stimulation current, and  $S_i(t)$  represents recurrent network interactions. Whenever  $V_i(t)$  crosses the threshold value  $V_{T,i}$  neuron  $i$  sends a spike to its postsynaptic neighbors and  $V_i$  reverts to the neuron's reset potential  $V_{R,i} < V_{T,i}$ . The interaction between neurons within the network is hence represented by the weighted  $\delta$ -pulse function

$$S_i(t) = \sum_{j=1}^N \sum_{k \in \mathbb{N}} a_{ij} \delta(t - t_{j,k} - \tau_{ij}), \quad (2)$$

in which  $t_{j,k}$  denotes the  $k$ -th spike time of neuron  $j$ , and  $a_{ij}$  and  $\tau_{ij}$  are the synaptic coupling strength and the synaptic transmission delay of the connection  $j \rightarrow i$ , respectively.

If there are no recurrent interactions ( $S_i(t) \equiv 0$ ) and  $I_i$  is constant the solution of (1) for initial condition  $V_i(0) = V_{R,i}$  is given by

$$V_i(t) = R_i I_i (1 - e^{-\gamma_i t}) + V_{R,i} e^{-\gamma_i t}. \quad (3)$$

This implies that for  $R_i I_i > V_{T,i}$  (suprathreshold external current) the membrane potential is oscillating such that  $V_i(t + T_i) = V_i(t)$  with period

$$T_i = \frac{1}{\gamma_i} \ln \left( \frac{R_i I_i - V_{R,i}}{R_i I_i - V_{T,i}} \right). \quad (4)$$

The general solution of the non-autonomous inhomogeneous linear differential equation (1) for times  $t > t_0$  with initial condition  $V_i(t_0)$  is given by (cf. Arnold, 1992)

$$V_i(t) = R_i I_i (1 - e^{-\gamma_i (t-t_0)}) + V_i(t_0) e^{-\gamma_i (t-t_0)} + \sum_{j=1}^N \sum_{t_0 < t_{j,k} + \tau_{ij} \leq t} a_{ij} e^{-\gamma_i (t-t_{j,k}-\tau_{ij})}. \quad (5)$$

This solution, which holds for all times  $t > t_0$  until neuron  $i$  next experiences a threshold crossing, provides the basis for the reconstruction method described below.

It should be noted that the tractable nature of this model means that simulating networks of LIF neurons is straightforward. In particular, it can be efficiently and exactly done using standard event-based simulation techniques (Mattia and Giudice, 2000; Timme et al., 2003).

### 2.2 GENERAL RECONSTRUCTION METHODOLOGY

How can we obtain the interaction strengths  $a_{ij}$  for a particular neuron  $i$  and thus the network topology? The aim is to assemble multiple linearly independent instances of (5) into a linear system of rank  $N$  and solve for the unknown  $a_{ij}$  values. If the model parameters  $R_p$ ,  $V_{R,p}$ ,  $V_{T,p}$ ,  $\gamma_p$  and  $\tau_{ij}$  are known and the dynamical quantities

$t_0, t, V_i(t_0)$ , and  $V_i(t)$  are specified, equation (5) provides a restriction on the  $N$  input coupling strengths  $a_{ij}$  for a given neuron  $i$ . Choosing sufficiently many different values of the pairs  $t$  and  $t_0$  so as to provide linearly independent instances of (5) will therefore give  $N$  restrictions that fully determine all coupling strengths  $a_{ij}, j \in \{1, \dots, N\}$ . Repeated for each  $i$  this yields the entire network topology.

### Acceptable inter-spike intervals

We can use subsequent spike times  $t_0 = t_{i,\ell-1}$  and  $t = t_{i,\ell}$  to fix the dynamical quantities if they are chosen in an appropriate way. We first note that we can safely use any spike time to determine an initial condition, since post-spike the LIF neuron always immediately resets to voltage  $V_{R,i}$ . Hence our criterion for choosing an interval depends only on the way threshold crossings are induced, either by an incoming excitatory spike (*spike-induced* spiking) or by passive propagation due to sufficiently large driving  $I_i$  (*current-induced* spiking). For current-induced spiking the membrane potential  $V_i(t_{i,\ell}^-)$  of neuron  $i$  is known to be exactly at the threshold value  $V_{T,i}$ , while spike-induced spiking will generally supply excess depolarization such that the actual membrane potential will be at some unknown value  $V_i(t_{i,\ell}^-) > V_{T,i}$ . Hence if we restrict our choice of intervals  $(t_{i,\ell-1}, t_{i,\ell})$  to those terminating with current-induced spikes the following substitutions are valid in (5):

$$\begin{aligned} V_i(t_0) &:= V_i(t_{i,\ell-1}^+) = V_{R,i} \\ V_i(t) &:= V_i(t_{i,\ell}^-) = V_{T,i}. \end{aligned} \quad (6)$$

In order to find these intervals we must compare the spike times  $t_{i,\ell}$  of neuron  $i$  with all possible arrival times  $t_{j,k} + \tau_{ij}$  of all neurons  $j$ . To exclude intervals with potentially spike-induced spikes, we restrict the analysis to intervals where no  $t_{j,k} + \tau_{ij}$  coincides with the respective  $t_{i,\ell}$  and hence define the inter-spike interval  $(t_{i,\ell-1}, t_{i,\ell})$  as *acceptable* for neuron  $i$  if

$$t_{j,k} + \tau_{ij} \neq t_{i,\ell} \text{ for all } j \in \{1, \dots, N\}, k \in \mathbb{N}. \quad (7)$$

It is important to note two things: first, that we often have at our disposal many more than  $N$  acceptable intervals; and second, that not every set of  $N$  acceptable intervals will provide  $N$  linearly independent instances of (5). In particular, consecutive acceptable intervals might contain very similar arrival patterns, resulting in badly conditioned or even low-rank systems. Of course, there is no constraint to select only  $N$  intervals; if we use  $M > N$  intervals then the system will be formally overdetermined but solvable, though  $M \gg N$  is not favorable for efficiency reasons. Usually, selecting a subset of  $N$  or more intervals distributed across the respective incoming spike trains will be sufficient if the spiking is asynchronous and irregular (meaning that inter-spike interval correlations decrease quickly with time), the mean firing rate for all neurons is positive, and the spike recording is long-enough to find sufficiently many uncorrelated acceptable inter-spike intervals to derive  $N$  linearly independent instances of (5). In Section 3.1 various strategies for selecting subsets of acceptable intervals will be discussed. Note that we are not constrained to use spike train segments obtained under a single driving condition.

Assuming there are  $M \geq N$  acceptable intervals that will ensure linear independence, all presynaptic connections for neuron  $i$ ,  $A_i = (a_{i1}, \dots, a_{iN})$  are obtained in the following way: let  $D_{i,m} = (t_{i,\ell_m-1}, t_{i,\ell_m})$  be the  $m$ -th member of our subset of acceptable

inter-spike intervals, and  $T_{i,m} = t_{i,\ell_m} - t_{i,\ell_m-1}$  be the respective inter-spike interval of neuron  $i$ . We then define the  $M \times N$  matrix  $\Theta^{(i)}$  and the column vector  $B^{(i)}$  by

$$\Theta_{m,j}^{(i)} = \sum_{t_{j,k} + \tau_{ij} \in D_{i,m}} \exp(-\gamma_i [t_{i,\ell_m} - t_{j,k} - \tau_{ij}]) \text{ and} \quad (8)$$

$$B_m^{(i)} = V_{T,i} - R_i I_{i,m} (1 - e^{-\gamma_i T_{i,m}}) - V_{R,i} e^{-\gamma_i T_{i,m}}. \quad (9)$$

The incoming connectivity for neuron  $i$  is obtained by solving the linear system

$$\Theta^{(i)} A_i^\top = B^{(i)} \quad (10)$$

for  $A_i$ . Repeating the procedure for each neuron  $i \in \{1, \dots, N\}$  separately yields all  $N$  rows of the coupling matrix  $A$ , and thus the entire synaptic connectivity of the network.

### 2.3 RECONSTRUCTION IN THE PRESENCE OF SIMPLE PERIODIC SPIKING

The method described above can be applied to a broad range of spiking patterns and does not rely on network synchronization, phase-locking, or other steady state requirements. Since repeated spike patterns within the inter-spike intervals will lead to linear dependent rows in the derived  $\Theta$  matrix (8), systems that do exhibit phase-locked dynamics may require special handling. For excitatory and mixed systems it is usually sufficient to use heterogeneous driving currents  $I_p$  e.g., randomly drawn from some distribution  $\mathbb{P}(I)$ , with a variance large enough to perturb the system out of any phase-locked state. Certain inhibition dominated LIF networks exhibit stable dynamics even under a wide range of heterogeneous drivings. Inhibitory networks where  $a_i \equiv \sum_j a_{ij} < 0$  and  $0 < (\max_i a_i - \min_i a_i) < \tau_{ij}$  will generate stable phase-locked states with common period  $T$  when stimulated with a homogeneous current  $I_i = I$  (Denker et al., 2004). When  $a_i = a < 0$  for each  $i$  the system will also be able to consistently achieve stability under heterogeneous driving conditions, since the spread of the spike pattern is solely caused by the spread  $\Delta I_{i,m} \equiv \max_i I_{i,m} - \min_i I_{i,m}$  of the driving currents. This last subclass of networks we will denote as *homogeneous inhibitory*.

Homogeneous inhibitory LIF networks typically exhibit *simple periodic spike patterns*, i.e., all neurons fire exactly once before the same spike pattern repeats. If the neurons fire in a simple periodic pattern such that for any given inter-spike interval  $t_{i,\ell-1}, t_{i,\ell}$  each neuron  $j \neq i$  spikes exactly once within  $(t_{i,\ell-1} - \tau_{ij}, t_{i,\ell} - \tau_{ij})$ , each acceptable interval contains a complete set of representative arrivals, and (5) simplifies to

$$V_{T,i} = R_i I_i (1 - e^{-\gamma_i (t_{i,\ell} - t_{i,\ell-1})}) + V_{R,i} e^{-\gamma_i (t_{i,\ell} - t_{i,\ell-1})} + \sum_{j=1}^N a_{ij} e^{-\gamma_i (t_{i,\ell} - t_j - \tau_{ij})} \quad (11)$$

for all  $i \in \{1, \dots, N\}$ .

In order to guarantee linear independence it is necessary to gather data from multiple, relatively short spike trains obtained under varied driving conditions  $I_{i,m}, m \in \{1, \dots, N\}$  (cf. Timme, 2007) which additionally satisfy  $\forall_{i,j} i \neq j \Rightarrow I_{i,m} \neq I_{j,m}$ . If a network is able to achieve periodic simple spike patterns under each of these drivings then all intervals after the initial transient period are acceptable with identical or close to identical arrival patterns, hence we can always choose the last intervals recorded to solve the  $N$  linear systems (5). This means

that although this type of network dynamics makes it mandatory to repetitively drive the system with independent sets of currents, it spares us the necessity of scanning the spike data for acceptable intervals and so allows for fast reconstruction. We will refer to this case as the *specialized method* for homogeneous inhibitory networks.

### 3 IMPLEMENTATION AND PERFORMANCE

#### 3.1 ACCEPTABLE INTERVAL SEARCHES

For LIF networks other than the homogeneous inhibitory networks described in Section 2.3, spike patterns will almost always be asynchronous rather than simple periodic; hence we must actively search through spike trains for acceptable intervals.

In principle, if a full-rank system is embedded in the data then only  $N$  intervals are required, some of which may contain zero or more than one representative  $t_{jk} + \tau_{ij}$  value. One alternative to trying to identify such a minimum set of intervals would be to select  $M > N$  intervals according to some criterion which either guarantees or at least maximizes the chance that we have a full-rank subset; we could, for example, select *all* available acceptable intervals. Similarly, if we have  $M > N$  intervals we have the choice of solving the overdetermined  $M \times N$  system by, e.g., a least-squares method, or aggregating instances of (5) to patch together an  $N \times N$  system.

In our implementation we used independent partial scans of spike train segments to collect  $M \geq N$  intervals; the scans use the heuristic described below to construct a full-rank system if possible

while reducing search time and keeping  $M$  reasonably close to  $N$ . Multiple intervals found in close proximity are combined to create exactly solvable  $N \times N$  systems, since they are preferable to overdetermined systems in terms of both time requirements and numerical stability.

Within segments, our search strategy is based on a minimum-scan-length policy. Given data segments  $S_m, m \in \{1, \dots, N\}$ , then for each neuron  $i$  each segment  $S_m$  is scanned only as far as needed to obtain representative  $t_{jk} + \tau_{ij}$  values for all neurons  $j$ , and intervals are only chosen if they contributed a new member to the representative set. Instances of (5) for the intervals are then summed to become the  $m$ -th row of the solution matrix  $\Theta^{(i)}$  and  $m$ -th element of the vector  $B^{(i)}$ . When particular representatives are not present in particular segments then corresponding  $\Theta_{m,j}^{(i)}$  elements are set to zero. Balancing representatives by requiring a full set for each row and excluding redundancies is more than we technically require, but in practice this results in better conditioned  $\Theta^{(i)}$  matrices and hence more accurate results.

#### 3.2 ACCURACY OF THE BASIC METHOD

We first analyze the performance of the method for full-rank systems without additional noise or uncertainty. As shown in **Figure 1**, the reconstruction error is negligible, both for networks with phase-locked spike patterns as well as those with irregular spiking. The numerical error that appears in the reconstructions is solely the

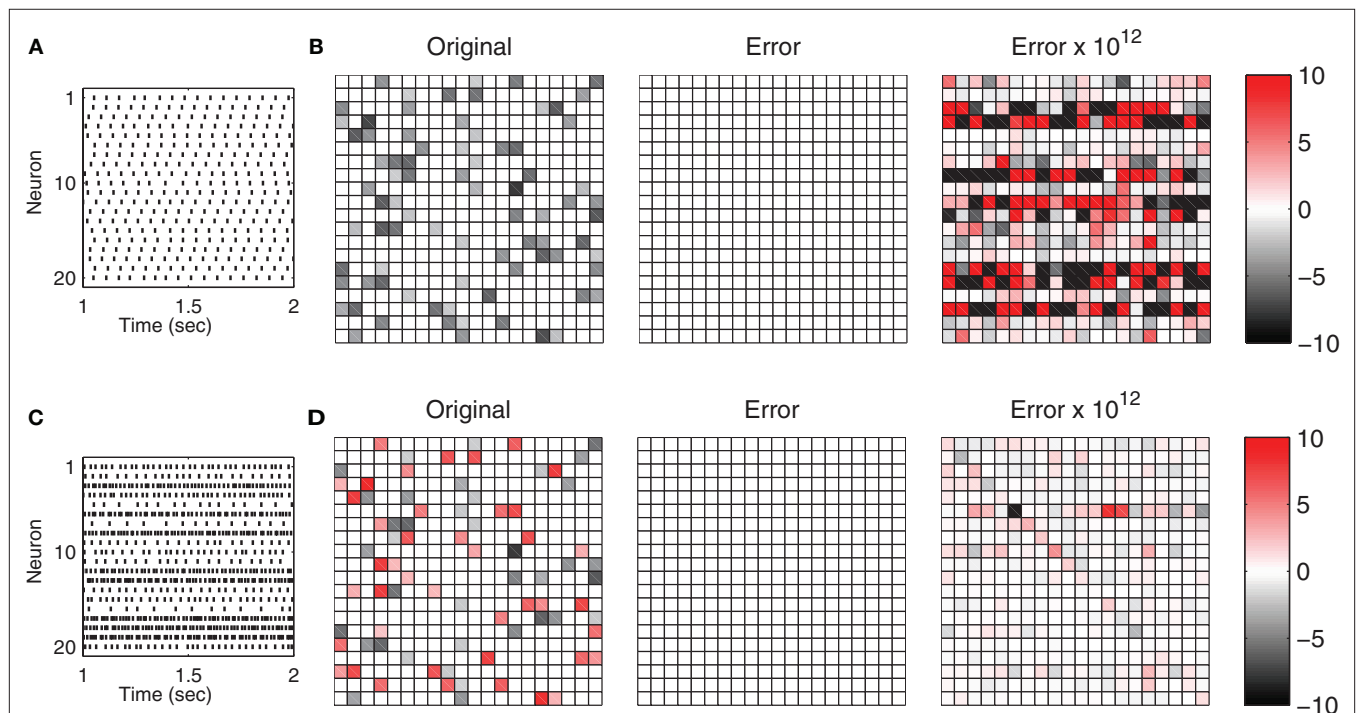


**FIGURE 1 | Topology reconstruction from simple periodic and complex aperiodic spike patterns. (A)** Simple periodic spike pattern of an inhibitory network. **(B)** Connection weights of the same network, with full-rank reconstruction error  $a_j - \hat{a}_j$ , and its magnification; strengths and errors are color coded on same scale. Error is on the level of numerical accuracy. **(C)** Complex spatio-temporal spike pattern of a heterogeneous network with both inhibitory and excitatory connections.

**(D)** Connection weights and error for the heterogeneous network. Both networks share the same underlying adjacency structure; the heterogeneous network was obtained from the inhibitory network by randomly changing the signs of connections with probability  $p = 0.5$ . Simulation parameters for both systems (uniform for all neurons): external driving  $\gamma_i R_i I_i = 1$  mV/ms with uniform random variation  $\Delta I/I = 5\%$ ,  $1/\gamma_i = 31.64$  ms,  $V_{R,i} = 0$  mV,  $V_{T,i} = 20$  mV,  $\tau_{ij} = 5$  ms.



result of small truncation errors in the derived data being propagated through global operations such as matrix inversion. When the specialized version of the method is used on phase-locking networks, this error level is as well directly and linearly dependent on the degree of synchronization experienced by the network (see **Figure 3**). As the exit tolerance is decreased this tunable error meets a hard limit where the truncation is no longer caused by early termination of the simulation, but instead by the fixed-precision numbers used by the machine the calculations are performed on. It should be noted that (apart from their influence on the network's ability to synchronize) the magnitude of simulation parameters does not affect the accuracy of the results in any noticeable way.

Since the general reconstruction method does not depend on synchronization, for data characterized by sustained irregular or chaotic spiking the entire error can be attributed to fixed-precision effects. A necessary precondition for achieving this level of accuracy

is of course that enough data be made available. As **Figure 2A** shows, the minimum number of intervals required to achieve full accuracy is not large; roughly 7 or 8 per segment ( $\approx 160$  total) for a 20-neuron network, for example. Whether data is obtained from  $N$  independent drivings or from a single run does not as well seem to have a large effect; sampling out of a very long run does reduce the minimum requirement by an interval or two, but the amount of data that must be generated in the first place to achieve this effect is appreciably greater. Compare also the specialized method featured in **Figure 3**, where the data requirement is exactly one interval per segment, but to achieve, e.g.,  $10^{-10}$  accuracy each segment needs to be  $\approx 60$  intervals long.

Independent of the driving conditions applied, there is no prior constraint on network configurations solvable by the methodology, aside from the assumption that  $a_{ij} < V_{T,i} - V_{R,i}$  i.e., that no single spike can move the membrane potential from reset to threshold. In

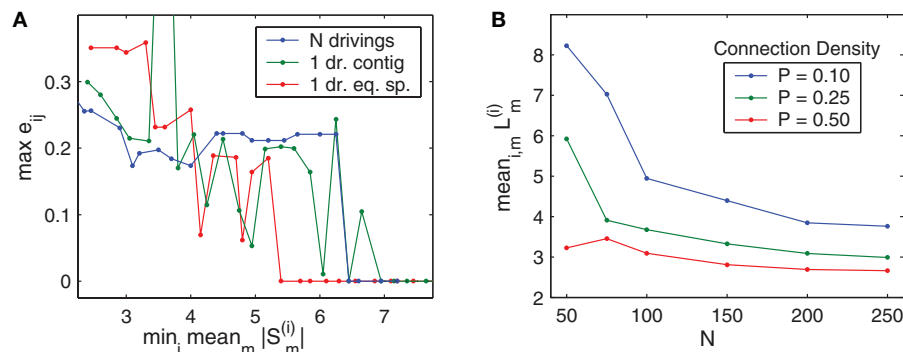


**FIGURE 2 | Reconstruction accuracy for complex spatio-temporal patterns as affected by search requirements. (A)** Maximum reconstruction error  $e_{ij} = |a_{ij} - \hat{a}_{ij}|$  vs. data availability as measured by segment length (in spikes) for slowest neuron. Different curves compare effect of data source: (blue) segments obtained under  $N$  different drivings, (green) contiguous segments taken from one run of moderate length, or (red) segments taken at equally spaced intervals from a long run (roughly 1000 spikes per neuron in this case). Runs use the same sample

network and parameters as shown in **Figures 1C,D**. **(B)** Interval search length  $L$  using min-scan-length strategy vs. size of network  $N$  for different connection densities  $P$ . Note: all reconstructions here achieved the numerical limit of accuracy. Simulation parameters: balanced networks ( $\sum_j a_{ij} = 0$ ) with no other restriction on pre- or postsynaptic connectivity, data obtained under  $N$  uniformly randomized driving conditions, base driving  $\gamma_i R_{T,i} = 1.5$  mV/ms,  $\Delta I/I = 1\%$ ;  $\tau_{ij} = 2$  ms,  $1/\gamma_i = 20$  ms,  $V_{R,i} = 0$  mV,  $V_{T,i} = 20$  mV (uniform for all neurons).

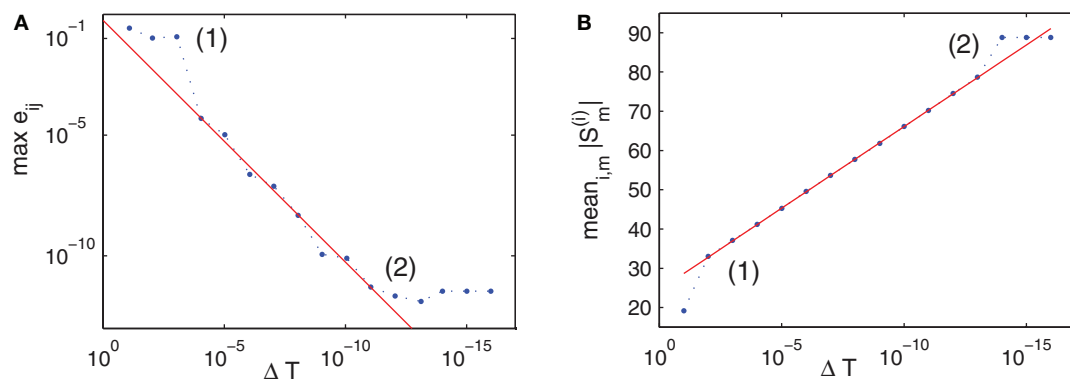


**FIGURE 3 | Reconstruction accuracy for phase-locking networks as affected by periodicity. (A)** Maximum reconstruction error  $e_{ij} = |a_{ij} - \hat{a}_{ij}|$  vs. phase-locking as measured by exit tolerance  $\Delta T$ , the maximum difference between final period lengths of different neurons. **(B)** Length of simulation

runs  $S_m$  (given as number of spikes emitted by neuron  $i$ ,  $|S_m^{(i)}|$ ) needed to achieve a specified  $\Delta T$ . Annotations: (1) indicates non-full-rank solutions due to insufficient synchronization; (2) indicates numerical saturation. Data is from sample network used for **Figures 1A,B**.

particular there are no other restrictions on the synaptic coupling strengths  $a_{ij}$ , or whether they are zero (no synapse present), positive (excitatory), or negative (inhibitory).

There is on the other hand no prior guarantee that any particular driving will give good results. In practice, randomly varied driving which satisfies  $R_{I,i} > V_{T,i}$  almost always gave us fully accurate reconstructions. There are two situations that can cause problems for the general method when otherwise long-enough data streams are made available: (i) quiescent neurons (no recoverable incoming or outgoing connections), and (ii) neurons for which all spiking throughout entire segments is spike-induced (outgoing connections recoverable, incoming connections not). Only (i) arose in our testing on random networks with random drivings, and never with networks subject to any kind of balance conditions, e.g.,  $|\sum_{j \in \text{inhib}} a_{ij}| \approx |\sum_{j \in \text{excit}} a_{ij}|$ . It should be noted that with respect to both situation (i) and situation (ii) the accuracy of reconstruction of the remainder of the network is not affected, and if needed both situations can be prevented by adjusting the driving to the relevant neurons.

### 3.3 EFFICIENCY

To check the speed of the methods we reconstructed networks of  $N = 50$  to  $N = 500$  neurons. As the range of  $N$  here implies, moderately sized networks (several hundred neurons) are still feasible for both the specialized and the general method; using the specialized method reconstruction of 250 neuron networks took about 1 min on a single node of a 4-CPU 2 GHz machine, while general reconstruction of the same network took about 20 min.

As these time ranges imply, the general method's reliance on data acquired from directly searching spike trains makes it noticeably slower than the specialized method in the size range tested here. This is in part due to the length of searches, but fixed costs for setting up the searches and computational platform were also factors (implementations were done in MATLAB, which is optimized for matrix operations but not generic search routines).

The worst case running time for the search phase of the general method is  $\mathcal{O}(S_{\max} N^3)$ , where  $S_{\max}$  is the length of the longest spike train. In practice most searches are not worst case; for the network of **Figure 1D**, for example, the mean segment length was 92 spikes, while the mean search length was 12 intervals and the mean number of acceptable intervals selected was around 3. As **Figure 2B** shows, the search length does not seem to increase as  $N$  grows but rather converges to a constant value; a similar effect is seen with the connection density (and hence the number of connections). We note that if situation (ii) mentioned in Section 3.2 occurs, the search time will in fact revert to the theoretical worst case.

After the search phase is completed, the algebraic operations require solving  $N$  individual  $N \times N$  linear systems, so they have a time complexity of  $\mathcal{O}(N^4)$  using conventional matrix inversion or Gaussian elimination. Hence, if the length of each neuron's spike train is bounded within  $\mathcal{O}(N)$  (i.e., each neuron spikes a fixed number of times for each neighbor) the worst case running time for the method as a whole is as well  $\mathcal{O}(N^4)$ . The numerical results shown in **Figure 1** suggest that this amount of data should generally be quite sufficient for accurate reconstruction. The implication is that the computational effort of reconstructing the structural

connectivity of spiking neural networks scales polynomially, and not exponentially, with network size. This is a significant finding concerning network reconstruction, since many other problems in bioinformatics are known or conjectured to be NP-complete, that is, for all intents and purposes intractable (cf. Foulds and Graham, 1982; Ngo et al., 1994).

### 3.4 EXPLOITING SPARSITY – SOLUTIONS FOR UNDERDETERMINED SYSTEMS

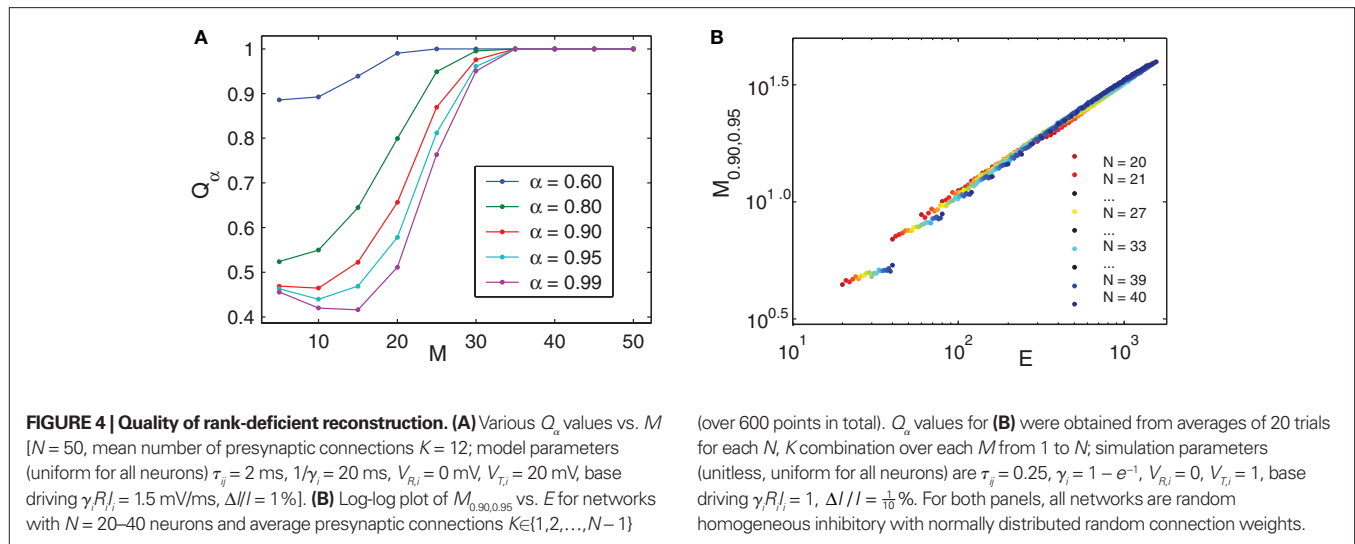
Recent studies (Yeung et al., 2002; Timme, 2007) used singular value decomposition  $USV^T = \Theta^{(i)}$  and optimization for sparsity to reconstruct with  $M \ll N$  distinct driving conditions. In general, this yields the underdetermined system  $A_i = \tilde{V} \tilde{S}^{-1} U^T B^{(i)} + Vx$  where  $\tilde{S}^{-1}$  is the pseudoinverse of  $S$  and  $x$  is any vector. Setting  $x = \bar{0}$  gives us the usual least-squares solution, but on the naturalistic assumption that neuronal network connectivity matrices  $A$  are sparse we can choose  $x$  so as to maximize the number of zeros in each  $A_i$ . To do this we use the heuristic of solving the overdetermined system  $Vx = -\tilde{V} \tilde{S}^{-1} U^T B^{(i)}$  for  $x$  so as to minimize the  $L_1$ -norm of the difference; our implementation uses the fast  $L_1$ -norm solver of Barrowdale and Roberts (1974).

Our primary interest is the lowest  $M < N$  we require to obtain sufficiently many reconstructed couplings  $\hat{a}_{ij}$  close enough to the corresponding elements of the original connectivity matrix  $a_{ij}$ , so that  $\hat{A}$  (after appropriate rounding) can be used as a plausible estimate for  $A$  in any hypothetical analysis. Hence along with the usual error measurements we also use a custom quality-of-fit metric,  $Q_\alpha^{(w)}(\hat{A})$ , that essentially yields the proportion of sufficiently close element-to-element matches, in this case for a given  $M$ :

$$Q_\alpha^{(w)}(\hat{A}) = w \frac{1}{|\text{nz}(A)|} \sum_{a_{ij} \neq 0} H \left( (1 - \alpha) - \frac{|\hat{a}_{ij} - a_{ij}|}{\max |A|} \right) + (1 - w) \frac{1}{|z(A)|} \sum_{a_{ij} = 0} H \left( (1 - \alpha) - \frac{|\hat{a}_{ij} - a_{ij}|}{\max |A|} \right) \quad (12)$$

The parameter  $\alpha$  is a value between 0 and 1 governing the desired per-element accuracy, e.g., an  $\alpha$  value of 0.80 means we want the proportion of elements in the reconstructed matrix that are within (roughly) 80% to 120% of the target value.  $\text{nz}(A)$  and  $z(A)$  are the sets of all non-zero and all zero elements of  $A$ , respectively, and  $H$  is the Heaviside step function. The weighting is incorporated to prevent false high scores when  $M$  is low and the target  $A$  is very sparse (cf. the original version of the quality measure in Timme, 2007). We exclusively used  $Q_\alpha^{(w)}$  with  $w = 0.5$ , which in the following we simply denote by  $Q_\alpha$ . **Figure 4A** shows a sampling of  $Q_\alpha$  values vs.  $M$ .

Networks with simple phase-locked spike pattern dynamics are solvable using the faster specialized method, so since a great many reconstruction computations were required these were used as our testbed. Comparison of interpolated values of  $Q_\alpha$  across different values of  $N$ ,  $M$ , the number of connections  $E$ , and other simulation parameters confirmed that the quality of reconstruction for  $M < N$  depends almost entirely on  $M/N$  and the edge density  $P = E/N^2$ . To determine the minimum  $M$  necessary to achieve a desired quality-of-fit we define



$$M_{q,\alpha} = \min_{1 \leq M \leq N} \{M : Q_\alpha(\hat{A}_M) \geq q\}. \quad (13)$$

The  $Q_\alpha$  profiles in **Figure 4A** show that there will be values of  $q$  for which  $Q_\alpha$  does not exist or is not unique. When both  $q, \alpha \geq 0.75$ , however,  $M_{q,\alpha}$  is well-defined and we consistently obtained relations of the form

$$M_{q,\alpha} \approx E^\beta + c \quad (14)$$

where scaling exponent  $\beta = \frac{1}{2} + \epsilon$ , with  $|\epsilon| \ll 1/2$  and  $c \ll E$ . A simple log-log fit of the data used for **Figure 4B**, for example, gives a scaling exponent of 0.504, with  $c$  below one. The overall result implies that we can expect  $M_{q,\alpha}$  to grow linearly with  $N$  when  $P$  is fixed, and roughly as  $\sqrt{P}$  when  $N$  is fixed.

For general spatio-temporal patterns we obtain similar results, though they are not as pronounced or consistent, and there seems to be a greater dependence on factors other than  $M$ ,  $N$ , and  $E$ , such as actual network parameters and specific spike pattern. The particular interval search strategy used has an influence as well. These intermingled technical issues require further theoretical and computational studies.

### 3.5 SPIKE TIMING VARIABILITY DUE TO NOISE AND UNCERTAINTY

In the previous subsections we have described the performance of the reconstruction method for exactly known model parameters and spike times. In such cases, when there is sufficient data available for a full-rank solution the accuracy is limited only by machine precision, demonstrating that reconstruction of large pulse-coupled networks from spike time data is in principle feasible.

For real world data one must deal with limitations in our knowledge of neuron parameters, and also uncertainties due to the noisiness of the system. Even if spike times themselves are accurately measured and correctly assigned to their respective source neurons, spike timing is an inherently noisy process with intrinsic contributions from, e.g., fluctuations in ion channel dynamics and dendritic integration, as well as extrinsic contributions from, e.g., synaptic failure and dependence

on the network state itself (Gerstner and Kistler, 2002). This leads to variability in both spike times as well as transmission delays, even under identical external conditions (Mainen and Sejnowski, 1995; van Steveninck et al., 1997; Destexhe et al., 2003).

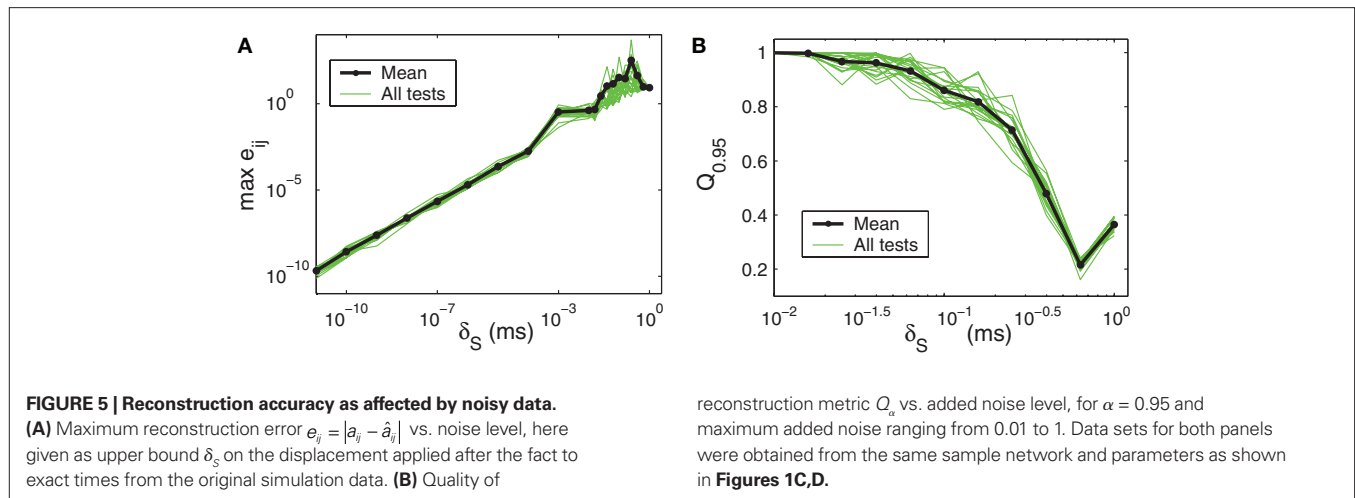
In this section we present some preliminary results concerning the performance of the reconstruction method when spike reception times are subject to additive random jitter bounded by an upper amplitude  $\delta_s$ . The presence of temporal jitter induces an uncertainty in comparison of spike times and estimated arrival times, and hence the identification of acceptable intervals [cf. (7)]. Given a spike by neuron  $j$  at  $t_{j,k}$ , if we naively try to apply the acceptable interval criterion in Section 2.2 to the jittered times  $\tilde{t}_{j,\ell} = t_{j,\ell} + \delta_{i,\ell}$  and  $\tilde{t}_{j,k} = t_{j,k} + \delta_{j,k}$ , then the interval as measured ( $\tilde{t}_{i,\ell-1}, \tilde{t}_{i,\ell}$ ) will very likely be erroneously accepted. Note that the measured/estimated time between the simultaneous arrival and spiking events is  $|\delta_{j,k} - \delta_{i,\ell}| \leq 2 \max\{|\delta_{j,k}|, |\delta_{i,\ell}|\} \leq 2\delta_s$ . As well, even if the interval is actually acceptable, arrivals close to both the initial spike time  $t_{i,\ell-1}$  and the terminal spike time  $t_{i,\ell}$  can cause inaccuracy by being wrongly assigned (or not assigned) to it. In order to exclude either case a new condition for the interval to be acceptable for neuron  $i$  has to be defined:

$$\forall j \in \{1, \dots, N\}, k \in \mathbb{N}: \tilde{t}_{j,k} + \tau_{ij} \notin [\tilde{t}_{i,\ell-1} - \epsilon, \tilde{t}_{i,\ell-1} + \epsilon] \cup [\tilde{t}_{i,\ell} - \epsilon, \tilde{t}_{i,\ell} + \epsilon], \quad (15)$$

with the uncertainty  $\epsilon$  depending on the noise amplitude  $\delta_s$ .

Without explicit knowledge of  $\delta_s$ , deciding on which  $\epsilon$  to choose is problematic: if too small there will be too many false positives, leading to large errors in the reconstruction; if too large many false negatives may lead to long interval searches, and in the worst case no acceptable intervals will be identified at all. As well, for fixed  $\delta_s$  and  $\epsilon$  simple probability dictates that increasing the network size will also increase the number of false negatives. This issue is a subject of future research.

**Figure 5A** shows how reconstruction accuracy (as given by the maximum absolute error) grows with uncertainty in the data, here implemented as jitter of amplitude  $\delta_s$  applied after the fact to



exact simulation data. The  $\epsilon$  used  $= 2 \max \delta_S$ . **Figure 5B** shows how our custom quality-of-fit metric  $Q_\alpha$  scales with applied noise as it approaches the model parameter values in magnitude. The  $\alpha$  value of 0.95 means that we are only considering a reconstructed element a hit when its value deviates from the target's by 5% or less. What may not be apparent from the log-log plot is that the decline in accuracy scales in a roughly linear way with the noise level, until the last point at 1.0 (this jog is an artifact of the  $Q_\alpha^{(w)}$  weighting used: the method can detect insufficient data and suppress untrustworthy results, but this feature was turned off for the error level tests; without the self-diagnostics, when there is no usable data whatsoever the method will return a uniformly zero matrix, which will generate correct matches for every non-connection in the original network).

Rank-deficient reconstruction as discussed in the previous subsection could be used to improve the accuracy of results for noisy systems. In our testing we have found that when  $M$  is close to but strictly less than  $N$ , application of SVD plus the  $L_1$ -norm solver acts as a numerical filter by forcing spurious low-grade connections toward zero strength. The optimal value for  $M$  in this case has yet to be determined (using  $M = N - 1$  usually gives very similar results to full-rank reconstruction). A potential application of the same principle is removing real but marginal connections from reconstruction results in order to obtain simpler connectivity patterns.

## 4 DISCUSSION

Understanding the relationship between structure and function of neuronal circuits lies at the very core of neuroscience. Modern recording devices, such as MUA that record the extracellular spike activity of tens to hundreds of neurons, provide time series whose interpretation can aid the understanding of the relevant functional connectivity and its spatial structure (cf. Aertsen and Gerstein, 1985; Aertsen et al., 1989; Berger et al., 2007, 2010, and others). Yet, to reconstruct the detailed connectivity of a neuronal network from recorded spike data is beyond recent data analysis techniques due to the complexities introduced by both individual neuron dynamics and network effects.

Here we have developed an explicit method for the reconstruction of network connectivity of LIF neurons from spike time information that is fast, accurate, and robust. The method works natively on networks exhibiting non-stationary complex spatio-temporal

dynamics (i.e., “plain” irregular spiking, Section 2.2); to solve networks with strong synchronizing tendencies it can, for example, make use of multiple randomized external driving conditions. A specialization of the method allows it to very efficiently reconstruct networks exhibiting simple spike patterns (Section 2.3), a dynamics that is reliably generated by a large subset of uniformly inhibitory LIF networks. This class is often used as a stand-in for inhibition dominated cortical networks (cf. Brunel and Hakim, 1999; Denker et al., 2004; Jahnke et al., 2009).

The general method is capable of reconstructing networks with several hundred neurons and arbitrary connectivity in a reasonable time given standard computational resources. In this regard the methodology compares favorably with reconstruction methods previously put forward for neuron networks (Makarov et al., 2005) and oscillator networks (Yu et al., 2006). Furthermore, the method is amenable to an optimization used earlier with reconstruction techniques for networks with fixed point dynamics (Yeung et al., 2002) and periodic dynamics (Timme (2007), cf. also Napoletani and Sauer (2008)) that substantially reduces the amount of data required.

The method introduced here is one of the first to achieve synapse-level reconstructions working from spike-based data, and it extends recoverability of pulse-based networks far beyond previously accessible sizes. However, as it currently stands, it does have its limitations that need to be addressed by future research if it is to be applied to biologically realistic data. To begin with, it is model dependent, and has to be given fixed known parameter values, even though these values need not be the same for every neuron in the network. As well, the method requires injection of external currents to individual neurons with a precision not yet generally achievable in an experimental setting (Houweling et al., 2010), nor will it work with externally undriven or weakly driven systems. While with some modification it can handle bounded amounts of noise and/or uncertainty, it is sensitive to errors with respect to, e.g., spike sorting.

Neuron models with more realistic spike generation mechanisms are worth further analysis within the response-dynamics idea that underlies our methodology. Possible extensions include: the *spike-response* model, a modification of the LIF neuron that incorporates refractoriness (Gerstner and Kistler, 2002); the two variable *adaptive exponential integrate-and-fire* neuron, which is capable of



a much wider range of individual neural behavior (bursting, fast, and slow mode, etc., cf. Brette and Gerstner, 2005); and further non-linear models such as the *quadratic integrate-and-fire* neuron (Izhikevich, 2007). Ultimately, the general aim is that a single algorithm contains the specifications for a repertoire of different models, which can be adapted to particular self-contained networks or also parts of networks, given an input model that mimics the residual large-scale network or upstream input areas. Since all available recording techniques have to deal with the general problem of undersampling, both with regard to the number of neurons as well as with regard to the finite time a stable recording is possible, minimizing the data required for desired accuracy is an important feature of any potentially useful reconstruction algorithm.

The method presented here is not designed to replace large-scale correlation-based methods, as functional connectivity continues to be the main approach to reconstruction problems in neuroscience. However, to determine the details within the regions of interest that functional connectivity studies identify will require methods

that can provide data on the scale of individual synaptic connections. The complexity analysis provided in Section 3.3 shows for the first time that reconstruction based on spike pattern information is computationally feasible. If explicit methods such as the one presented here can be developed to work on large-scale networks with appropriate biophysical neuron models, they may become invaluable in these studies. Thus we see our methodology as an eventual complement to techniques currently in use, providing a promising starting point for future research of neural circuit inference from spiking activity.

## ACKNOWLEDGMENTS

We thank Sara Solla and Fred Wolf for helpful comments. We also thank Christian Henrich for his contributions in the early stages of this work, and Zeina S. Khan for her careful reading of the manuscript. We acknowledge funding by the Federal Ministry of Education and Research (BMBF) Germany for partial support under Grant No. 01GQ1005B.

## REFERENCES

- Aertsen, A., and Gerstein, G. L. (1985). Evaluation of neuronal connectivity: sensitivity of cross-correlation. *Brain Res.* 340, 341–354.
- Aertsen, A., Gerstein, G. L., Habib, M. K., and Palm, G. (1989). Dynamics of neuronal firing correlation: modulation of “effective connectivity.” *J. Neurophysiol.* 61, 900–917.
- Arnol'd, V. I. (1992). *Ordinary Differential Equations* (R. Cooke, trans.). Berlin: Springer-Verlag.
- Barrowdale, I., and Roberts, F. D. K. (1974). Algorithm 478: solution of an overdetermined system of equations in the  $l_1$  norm [F4]. *Commun. ACM* 17, 319–320.
- Berger, D., Borgelt, C., Louis, S., Morrison, A., and Grün, S. (2010). Efficient identification of assembly neurons within massively parallel spike trains. *Comput. Intell. Neurosci.* 2010, 439648.
- Berger, D., Warren, D., Normann, R., Arieli, A., and Grün, S. (2007). Spatially organized spike correlation in cat visual cortex. *Neurocomputing* 70, 2112–2116.
- Brette, R., and Gerstner, W. (2005). Adaptive exponential integrate-and-fire model as an effective description of neuronal activity. *J. Neurophysiol.* 94, 3637–3642.
- Brunel, N. (2000). Dynamics of sparsely connected networks of excitatory and inhibitory spiking neurons. *J. Comput. Neurosci.* 8, 183–208.
- Brunel, N., and Hakim, V. (1999). Fast global oscillations in networks of integrate-and-fire neurons with low firing rates. *Neural Comput.* 11, 1621–1671.
- Cadenasso, M. L., Pickett, S. T. A., and Grove, J. M. (2006). Dimensions of ecosystem complexity: heterogeneity, connectivity, and history. *Ecol. Complex.* 3, 1–12.
- Denker, M., Timme, M., Diesmann, M., Wolf, F., and Geisel, T. (2004). Breaking synchrony by heterogeneity in complex networks. *Phys. Rev. Lett.* 92, 074103.
- Destexhe, A., Rudolph, M., and Pare, D. (2003). The high-conductance state of neocortical neurons in vivo. *Nat. Rev. Neurosci.* 4, 739–751.
- Diesmann, M., Gewaltig, M.-O., and Aertsen, A. (1999). Stable propagation of synchronous spiking in cortical neural networks. *Nature* 402, 529–533.
- Foulds, L., and Graham, R. (1982). The Steiner problem in phylogeny is NP-complete. *Adv. Appl. Math.* 3, 43–49.
- Gerstner, W., and Kistler, W. (2002). *Spiking Neuron Models: Single Neurons, Populations, Plasticity*. Cambridge, UK: Cambridge University Press.
- Houweling, A., Doron, G., Voigt, B., Herfst, L., and Brecht, M. (2010). Nanostimulation: manipulation of single neuron activity by juxtacellular current injection. *J. Neurophysiol.* 103, 1696–1704.
- Izhikevich, E. (2007). *Dynamical Systems in Neuroscience: The Geometry of Excitability and Bursting*. Cambridge, MA: The MIT Press.
- Jahnke, S., Memmesheimer, R.-M., and Timme, M. (2009). How chaotic is the balanced state? *Front. Comput. Neurosci.* 3:13. doi: 10.3389/fncom.2010.013.2009
- Jirsa, V. K., and McIntosh, A. R. (eds). (2007). *Handbook of Brain Connectivity*. Berlin: Springer.
- Mainen, Z., and Sejnowski, T. (1995). Reliability of spike timing in neocortical neurons. *Science* 268, 1503–1506.
- Makarov, V. A., Panetsos, F., and de Feo, O. (2005). A method for determining neural connectivity and inferring the underlying network dynamics using extracellular spike recordings. *J. Neurosci. Methods* 144, 265–279.
- Mattia, M., and Giudice, P. (2000). Efficient event-driven simulation of large networks of spiking neurons and dynamical synapses. *Neural Comput.* 12, 2305–2329.
- Napoletani, D., and Sauer, T. (2008). Reconstructing the topology of sparsely connected dynamical networks. *Phys. Rev. E* 77, 026103.
- Ngo, J., Marks, J., and Karplus, M. (1994). “Computational complexity, protein structure prediction, and the Levinthal paradox,” in *The Protein Folding Problem and Tertiary Structure Prediction*, eds K. Merz and S. Le Grand (Boston: Birkhauser), 433–506.
- Timme, M. (2007). Revealing network connectivity from response dynamics. *Phys. Rev. Lett.* 98, 224101.
- Timme, M., Wolf, F., and Geisel, T. (2002). Coexistence of regular and irregular dynamics in complex networks of pulse-coupled oscillators. *Phys. Rev. Lett.* 89, 258701.
- Timme, M., Wolf, F., and Geisel, T. (2003). Unstable attractors induce perpetual synchronization and desynchronization. *Chaos* 13, 377–387.
- van Steveninck, R., Lewen, G., Strong, S., Koberle, R., and Bialek, W. (1997). Reproducibility and variability in neural spike trains. *Science* 275, 1805–1808.
- van Vreeswijk, C., and Sompolinsky, H. (1996). Chaos in neuronal networks with balanced excitatory and inhibitory activity. *Science* 274, 1724–1726.
- Yeung, M. K. S., Tegnér, J., and Collins, J. J. (2002). Reverse engineering gene networks using singular value decomposition and robust regression. *Proc. Natl. Acad. Sci. U.S.A.* 99, 6163–6168.
- Yu, D., and Parilitz, U. (2008). Driving a network to steady states reveals its cooperative architecture. *Europhys. Lett.* 81, 48007.
- Yu, D., Righero, M., and Kocarev, L. (2006). Estimating topology of networks. *Phys. Rev. Lett.* 97, 188701.
- Zillmer, R., Brunel, N., and Hansel, D. (2009). Very long transients, irregular firing, and chaotic dynamics in networks of randomly connected inhibitory integrate-and-fire neurons. *Phys. Rev. E* 79, 031909.

**Conflict of Interest Statement:** The authors declare that the research was conducted in the absence of any commercial or financial relationships that could be construed as a potential conflict of interest.

Received: 14 May 2010; accepted: 10 January 2011; published online: 01 February 2011.

Citation: Van Bussel F, Kriener B and Timme M (2011) Inferring synaptic connectivity from spatio-temporal spike patterns. *Front. Comput. Neurosci.* 5:3. doi: 10.3389/fncom.2011.00003

Copyright © 2011 Van Bussel, Kriener and Timme. This is an open-access article subject to an exclusive license agreement between the authors and Frontiers Media SA, which permits unrestricted use, distribution, and reproduction in any medium, provided the original authors and source are credited.